Evaluation and Comparison of Image Quality for Indirect Flat Panel Systems with CsI and GOS Scintillators

Mehmet E. Aksoy[a], Mustafa E. Kamasak[b], Erkan Akkur[c], Ayhan Ucgul[d], Muzaffer Basak[d], Huseyin Alaca[a]

[a] Istanbul Health Directorate

[b] Istanbul Technical University, Faculty of Computer and Informatics

[c] Directorate General of Health for Border and Coastal Areas

[d] Sisli Etfal Research Hospital

Abstract

Aim: The objective of this study is to compare the image quality of flat panel systems that have cesium iodide (CsI) and gadolinium oxysulfate (GOS) scintillators in their detectors.

Method: CDRAD 2.0 phantom and CDRAD analyzer software is used for objective evaluation and comparison of image quality of flat panel systems with CsI and GOS scintillators. The image quality is investigated in terms of contrast and detail. Nine different flat panel systems from 6 different manufacturers are evaluated in this study. Four of these flat panels have CsI scintillators and the remaining 5 have GoS scintillators. For evaluations, 20 layers of plexiglass were placed on the top (10 layers) and bottom (10 layers) of the CDRAD 2.0 phantom to simulate a patient. 3 images were taken from each system at each dose level, which were analyzed by the CDRAD 2.0 analyzer software. Image qualities were investigated at four different dose levels (50, 100, 150, and 200 μGys). IQFinv is used as the quality metric.

Results: IQFinv values of GOS systems have little variance both within the same system and between all systems. On the other hand, CsI systems have higher variance in IQFinv values within the same system and between the systems. In addition, same CsI detectors (same model from the same manufacturer) used in different systems resulted in considerably different IQFinv values. CsI systems demonstrate 4-5 times more improvement in IQFinv value with increasing dose levels compared to GOS systems. Finally, IQFinv values of CsI systems are higher than GOS systems with statistically significance ($p<0.029$).

Keywords: diagnostic image quality, digital radiography, radiation dose, scintillators

1 Introduction

Digital radiography (DR) systems are gradually replacing the analog and computed radiography (CR) systems. Higher costs of the newer technology have to be justified in terms of higher image quality and/or lower patient dose. With the flat panel detectors, compact and mobile DR systems are produced. Flat panels are also produced with different detector technologies. Advance quality metrics are used to assess image quality of digital detectors such as modulation transfer function (MTF), detector quantum efficiency (DQE) etc. [1]. However, potential customers are also interested in the image quality of the overall systems. In a DR system, there are factors –beside the detector– that determine the image quality such as image processing software, x-ray generator stability etc. Therefore beyond advanced quality metrics, simpler metrics are required to measure the image quality of the overall imaging system.

The aim of this work is to compare image quality of overall flat panel DR systems that have cesium iodide (CsI) and gadolinium oxysulfate (GOS) scintillators in their detectors at different dose levels. Although it is known in general that CsI scintillators are superior compared to GOS scintillators, this has not been investigated quantitatively. Therefore, quantitative image quality analysis for the overall flat panel systems is aimed. In addition, a protocol for image quality measurement of a flat panel system is demonstrated. The protocol and metric results will provide benchmarks for potential customers. As the objective of this study is to compare different scintillator types, the manufacturer names are not given.

1.1 Flat Panel Detector Systems

According to their x-ray sensing mechanism, flat panel detectors can be divided into two categories: indirect and direct detectors. Indirect detector systems convert x-ray into visible light, and light charges photodiode array which are then read using thin-film transistors (TFT). On the other hand, direct detector systems convert x-ray to electronic signal without any intermediate conversion.

Different types of scintillators are used in indirect systems. Most commonly used scintillators are structured cesium iodide (CsI) and unstructured gadolinium oxy-

sulfate (Gd_2O_2S - GOS). Thicker layers of scintillator increase the amount of x-ray conversion to visible light and leading to good absorption efficiency. However, thick layers of scintillators increase the amount of scatter which decreases the constrast. On the other hand, thin scintillator layers have lower absorption efficiency but better spatial resolution.

CsI scintillators have parallel and discrete needle structured crystals that are approximately 5-10 μm wide. These needle structures form a channel to the photodiode layer and allow construction of thicker layers without contrast deterioration. GOS scintillators have unstructured granular phosphor screen that are the same type of phosphor used in the conventional intensifying screens. GOS have a disadvantage about low efficiency at high temperatures [2–4]. In addition, overall light output is better for CsI scintillator, as compared to GOS [4, 5].

1.2 Image Quality Assessment

There are many studies that evaluate the image quality of different radiographic systems. These studies compare different types of radiographic imaging technologies and systems against each other using subjective and/or objective methods. Bacher compared the image quality of screen-film, CR, and the indirect/direct flat panel systems in terms of effective dose in patient and contrast-detail detectability [6]. CDRAD 2.0 and CDMAM 3.4 phantoms were used in this study as the contrast-detail phantom [6]. In another study by Lu et. al, CR and screen-film systems are compared in terms of patient dose and contrast-detail curves [7]. M. A. Irvine compared the indirect flat panel systems and the CR in pediatric imaging in terms of image quality and radiation dose [8]. In other studies, flat panel, CR and screen-film systems are compared using image quality metrics such as modulation transfer function (MTF), noise power spectrum (NPS), and detective quantum efficiency (DQE) [9, 10]. Samei focused on evaluating the performance of CR and flat panel systems in terms of noise characteristic and affecting sharpness of the digital detector [11]. The effects of scintillator on the DQE of a CCD based digital system were compared by Farman et. al [12].

For the objective analysis of the image quality in digital radiology, a contrast-detail phantom has typically been used [6, 7, 13]. In the recent studies, the CDRAD 2.0 phantom has been used for image quality evaluation. CDRAD 2.0 phantom tests the observers perception. Using this phantom, it is possible to quantify the amount of detail and contrast observed by the observer. The results are given in a contrast-detail curve [6–8, 13–17].

There are two main disadvantages of subjective testing with observers: The results of the observer readings may show high variance (depending on the observers) and the results may not be reproducible. In addition, the reading process is time consuming. The disadvantages can be solved by objective tests, where software analyzes the images and applies statistical methods to determine contrast detail curves.

2 Materials and Methods

2.1 The CDRAD 2.0 contrast-detail phantom description

The CDRAD 2.0 phantom is constructed on a Plexiglas tablet (26.5 cm.×26.5 cm.× 1 cm.) (see Figure 1). 225 cylindrical holes of varying diameters and depths are drilled on this tablet. The depths and diameters of holes are sized from to 0.3 to 8.0 mm. The x-ray image will have 225 squares placed on a 15x15 grid. In the rows of the grid, the contrast (the depth of the holes) increases from left to right. In the columns of the grid, the diameter of the holes decreases from top to bottom. In the first 3 rows, there exists a single hole within each square. After the 3rd row, each square has two holes: one in the middle of the square and another in one of the four possible corner of the square. The holes are placed in random corners of the squares and patterns are avoided to mislead the observers [6, 17].

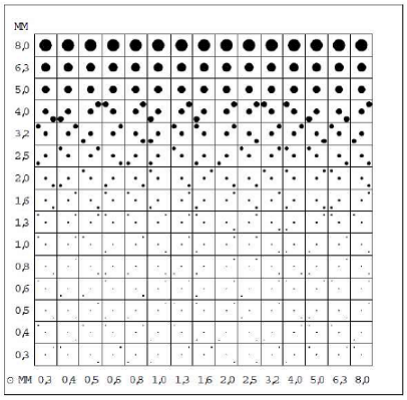

Figure 1: Schematic representation of the CDRAD 2.0 phantom.

2.2 CDRAD Analyzer

The CDRAD Analyzer software is developed by the manufacturer of CDRAD phantom [16]. It uses statistical methods to determine whether a certain contrast-detail combination is detected or not. Standard deviation and average pixel value of the image are used in the statistical methods. CDRAD Analyzer gives two metrics for image quality [16]. Correct observation ratio is the percentage of the correctly observed squares (the corner of the hole is correctly identified) to the total number of squares. The equation for correct observation ratio is:

$$\text{Correct observation ratio} = \frac{\text{Correct observations}}{\text{Total number of squares}} \times 100 \quad (1)$$

The other metric is called the image quality figure (IQF), which is defined as:

$$IQF = \sum_{i=1}^{15} C_i \times D(i, th) \ , \quad (2)$$

where $D(i, th)$ denotes the smallest diameter that is correctly observed (shown at each row in Figure 1) and C_i denotes the value in the contrast column (shown under each column in Figure 1) that corresponds to $D(i, th)$. As image quality and IQF are inversely proportional, an inverse image quality figure ($IQFinv$) is introduced:

$$IQFinv = \frac{100}{\sum_{i=1}^{15} C_i \times D(i, th)} \ . \quad (3)$$

IQFinv value increases with the image quality.

2.3 Image Acquisition

Images were collected from 9 different flat panel systems produced by 6 different manufacturers. To simulate the patient thickness (for solid organs in abdomen imaging) 10 plexiglass layers (PMMA) were placed on the top and another 10 PMMA were placed at the bottom (each layer is 26 cm x 26 cm x 1 cm) of the CDRAD 2.0 phantom as shown in Figure 2.

Source to detector (SSD) was set to 100 cm and automatic exposure control (AEC) was closed. The generator was set to 80 kVp in manual mode [6, 7, 14, 15, 17]. The mAs values were adjusted to obtain the entrance doses of 50μGy, 100μGy, 150μGy, and 200μGy. The achieved entrance dose was measured with dosimeter. For each system, the setup shown in Figure 3 is used to take 3 images at a certain entrance dose, and images are recorded in DICOM 3.0 format. The recorded images are analyzed by CDRAD 2.0 Analyzer. IQFinv values of these 3 images are computed and averaged to have a reliable estimate of IQFinv for a system at a specific dose. The average IQFinv value for each system can be plotted at different entrance doses for comparison [6, 13].

2.4 Data and statistical analyses

Phantom images were collected from 9 flat panel DR systems. For each system, 12 images (3 images/dose at 4 dose levels) of the phantom were taken. IQFinv values were computed for every image, and these values are averaged for each dose level. Therefore a single IQFinv value is computed for each system and dose level. Systems with GOS and CsI scintillators were compared at each dose level using Mann-Whitney U test [18]. The significance level was determined as 0.05 ($\alpha = 0.05$).

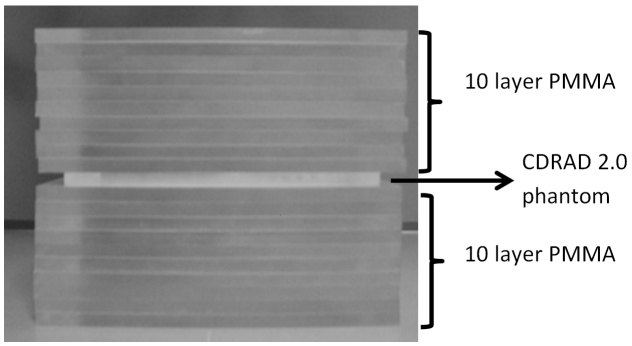

Figure 2: Phantom setup for image acquisition.

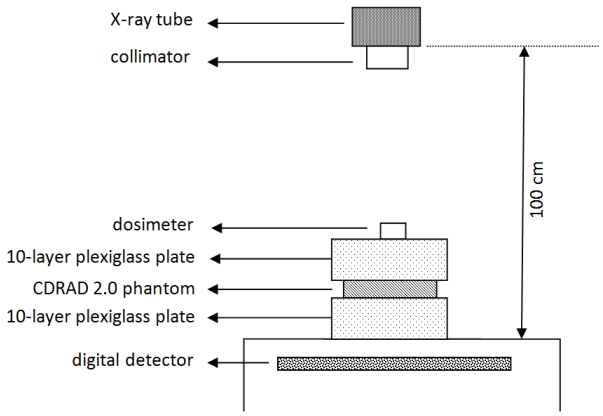

Figure 3: System setup for image acquisition.

3 Results

In the Figure 4 and Table 1, mean and standard deviation of IQFinv values corresponding to flat panel systems with GOS and CsI scintillators are given for different dose levels. All IQFinv values obtained from different GOS systems at different dose levels are listed in Table 2. Similarly, $IQFinv$ values for all CsI systems are given in Table 3.

In all systems, the $IQFinv$ values increased with the entrance dose. The relation between the entrance dose (μGy) and IQFinv for GOS and CsI systems are shown in Figure 5. Using linear regression, it was shown that the $IQFinv$ value increase faster for the CsI systems compared to the GOS systems.

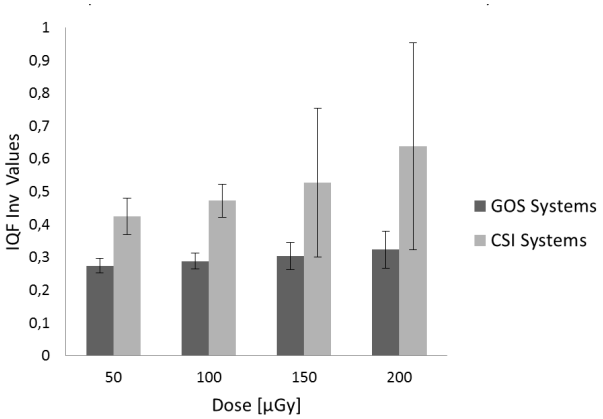

Figure 4: Comparison of flat panel DR systems with GOS and CSI scintillator.

Table 1: Mean and standard deviation of IQFinv values of GOS and CsI systems. These values are computed from IQFinv values given in Table 2 and Table 3.

	GOS Systems	
Dose [μGy]	Mean IQFinv	Std of IQFinv
50	0.275	0.022
100	0.288	0.023
150	0.304	0.042
200	0.324	0.056
	CsI Systems	
Dose [μGy]	Mean IQFinv	Std of IQFinv
50	0.425	0.055
100	0.472	0.049
150	0.527	0.227
200	0.639	0.316

4 Discussion

In Table 1 and Figure 1, mean and standard deviation of averaged IQFinv values among GOS and CsI systems are shown. The mean and standard deviations are computed from IQFinv values given in Table 2 and Table 3. Due to their common structure, detectors with GOS scintillators have similar image quality at different dose levels. From Table 2, it can also be observed that IQFinv values of images taken at a specific dose level show little variance within the same system and among all systems. At higher dose levels, the variance of IQFinv values within the same system is still low. On the other hand, the variance of IQFinv values among the systems starts to increase. However, the variance at higher dose levels is still low compared to the mean IQFinv value of the GOS systems.

CsI systems have similar IQFinv values at 50 and 100 μGys. However, their image quality differs at higher dose

Table 2: IQFinv values for GOS systems.

	GOS A			GOS B		
Dose [μGy]	IQFinv values			IQFinv values		
50	0.32	0.29	0.33	0.26	0.26	0.26
100	0.38	0.32	0.26	0.26	0.26	0.27
150	0.35	0.37	0.39	0.26	0.27	0.26
200	0.40	0.40	0.37	0.26	0.26	0.26
	GOS C			GOS D		
Dose [μGy]	IQFinv values			IQFinv values		
50	0.28	0.26	0.26	0.26	0.26	0.27
100	0.30	0.32	0.32	0.29	0.26	0.27
150	0.35	0.29	0.32	0.29	0.26	0.29
200	0.40	0.47	0.26	0.30	0.29	0.30
	GOS E					
Dose [μGy]	IQFinv values					
50	0.29	0.26	0.26			
100	0.29	0.26	0.29			
150	0.29	0.29	0.27			
200	0.30	0.30	0.29			

levels (ie. at 150 and 200 μGys). Table 3 gives IQFinv measurements of all CsI systems at different dose levels. From this table, it can be observed that the IQFinv values show higher variance compared to GOS systems within the same system at even low dose levels. As the dose increases beyond 100 μGy, the IQFinv variance both within the same system and between all systems is increased to a level approximately 50% of their IQFinv mean value. This indicates that the needle structure of CsI systems shows different performance to tunnel the visible light between image acquisitions at all dose levels. As the dose level increases, the difference between the systems become more substantial.

Some of the DR systems with both GOS and CsI scintillators evaluated in this study use the same flat panel detector (same model from the same manufacturer). However, their IQFinv values are different. This IQFinv difference for the same detector is more noticeable for CsI systems. Different image quality obtained from the same detector may be due to their image processing software and other system specifications.

For both GOS and CsI systems, the IQFinv values increases linearly with dose level. This relation is shown in Figure 5. From this figure, it is observed that CsI systems are approximately 4- 5 times more sensitive to dose level compared to GOS systems. In other words, the image quality of CsI systems improves more than GOS systems with the increasing dose level. This is an expected result as the DQE values of CsI scintillators are higher than GOS scintillators. The average IQFinv values of CsI and GOS systems are statistically compared. The difference between IQFinv values of these systems

Table 3: IQFinv values for CsI systems.

	CsI A			CsI B		
Dose [μGy]	IQFinv values			IQFinv values		
50	0.39	0.43	0.26	0.40	0.63	0.43
100	0.65	0.42	0.42	0.66	0.64	0.53
150	0.35	0.39	0.39	0.75	1.28	0.36
200	0.39	0.37	0.37	1.26	1.15	0.81
	CsI C			CsI D		
Dose [μGy]	IQFinv values			IQFinv values		
50	0.77	0.33	0.26	0.41	0.39	0.41
100	0.45	0.33	0.28	0.45	0.42	0.39
150	0.34	0.32	0.26	0.84	0.79	0.26
200	0.72	0.33	0.26	0.79	0.68	0.54

is statistically significant ($p<0.021$). In addition, the average IQFinv values of CsI systems are higher compared to GOS systems with statistical significance ($p<0.029$).

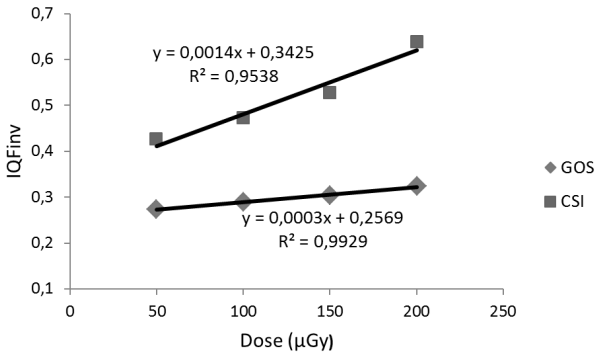

Figure 5: The relation between the entrance dose (μGy) and IQFinv for GOS and CsI systems.

5 Conclusion

In this study, CDRAD 2.0 phantom is used for objective evaluation of the contrast-detail characteristics of CsI and GOS scintillators. Nine different flat panel systems were used. Four of these flat panels had CsI scintillators and five had GOS scintillators. For each system, three images for each dose levels were taken. Four different dose levels (50, 100, 150, and 200 μGys) were investigated.

Systems with GOS scintillators show little variance within the same system and between all systems. On the other hand, system with CsI scintillator show higher variance within the same system and between the systems.

In addition, same detectors with CsI scintillators (same model from the same manufacturer) used in different systems resulted in considerably different $IQFinv$ values.

CsI systems demonstrate 4-5 times more improvement in $IQFinv$ value with increasing dose levels compared to GOS systems. This result is consistent with the DQE values of CsI and GOS scintillators.

Finally, $IQFinv$ values of flat panels systems with CsI scintillators are significantly higher than systems with GOS scintillator ($p<0.029$).

6 Acknowledgement

The authors would like to thank Prof. Nadir Arican (Istanbul University), Duygu Torun and Sezen Avtan (Istanbul Health Directorate) for their valuable discussions and contributions.

References

[1] Andrew G. Webb, editor. *Introduction to Biomedical Imaging*. Wiley-IEEE Press, 2002.

[2] P R Vaidya. Flat panel detectors in industrial radiography. Technical report, International Workshop on Imaging NDE, Kalpakkam, Chennai, India, April 2007.

[3] H G Chotas and C E Ravin. Digital chest radiography with a solid-state flat- panel x-ray detector: Contrast-detail evaluation with processed images printed on film hard copy. *USA Radiology*, 218:679–682, 2001.

[4] H K Kim, I A Cunningham, Z Yinn, and G Cho. On the development of digital radiography detectors: A review. *International Journal of Precision and Manufacturing*, 9(4):86–100, 2008.

[5] W Knupfer, E Hell, and D Mattern. Novel x-ray detectors for medical imaging. *Nuclear Physics*, pages 610–615, 1999.

[6] K Bacher. *Evaluation of Image Quality and Patient Radiation Dose in Digital Radiology*. PhD thesis, Faculty of Medicine and Health Sciences Department of Human Anatomy, Embryology, City, Country, 2006.

[7] Z F Lu, E L Nickoloff, J C So, and A K Dutta. Comparison of the computed radiology and film/screen combination using a contrast detail phantom. *Journal of Applied Clinical Medical Physics,*, 4(1):91–98, 2003.

[8] M A Irvine. Image quality and radiation dose comparison of a computed radiography system and an amorphous silicon flat panel system in pediatric radiography: A phantom study. Master's thesis, RMIT University, 2009.

[9] X Liu and C C Shaw. a-si:h/csi(tl)flat-panel versus computed radiography for chest imaging applications: Image quality metrics measurement. *Med. Phys.*, 31(1):98–111, 2004.

[10] C E Floyd, R J Warp, J T Dobbins, H G Chotas, A H Baydush, R Vargas-Vorecek, and C E Ravin. Imaging characteristics of an amorphous silicon flat-panel detector for digital chest radiography. *Med. Phys.*, pages 683–688, 2001.

[11] E Samei. Performance of digital radiographic detectors: Factors affecting sharpness and noise. *Advances in Digital Radiography: RSNA Categorical Course in Diagnostic Radiology Physics*, pages 49–61, 2003.

[12] T T Farman, R H Vandre, J C Pajak, S R Miller, A Lempicki, and A G Farman. Effects of scintillator on the detective quantum efficiency (dqe) of a digital imaging system. *Oral and Maxillo Facial Radiology*, 101:219–223, 2006.

[13] M McEntee, H Frawley, and P C Brennan. A comparison of low contrast performance for amorphous silicon/cesium iodide direct radiography with a computed radiography: A contrast detail phantom study. *Radiology*, 13:89–94, 2007.

[14] M Liaskos, C Michail, N Kalyvas, A Toutountzis, S Tsantis, G Fountos, D Cavouras, and I Kandarakis. Implementation of a software phantom for the assessment of contrast detail in digital radiography. *e-Journal of Science Technology(e-JST)*, pages 15–23, retreived 28.03.2011. http://e-jst.teiath.gr.

[15] K Bacher, P Smeets, L Vereecken, An De Hauwere, P Duyck, R De Man, K Verstraete, and H Thierens. Image quality and radiation dose on digital chest imaging: Comparison of amorphous silicon and amorphous selenium flat-panel systems. *Chest Imaging, AJR:187*, pages 630–637, September 2006.

[16] Artinis Medical System. *Manuals CDRAD 2.0 Phantom Analyzer Software version*, 2010.

[17] British Columbia [online database] Diagnostic Accreditation Program, Vancouver. Y11-dr digital radiography image quality. http://www.dap.org/CmsFiles/File/Safety Code HC35/Test Protocol Files/Y11DR.pdf. retrieved 20.06.2011.

[18] N Nachar. The mann-whitney u: A test for assessing whether two independent sample come from the same distribution. *Tutorials in Quantitative Methods for Psychology*, 4(1):13–20, 2008.